Metal-Free Organic Triplet-Emitters with On-Off Switchable Excited State Intramolecular Proton Transfer

Wenhao Shao[†], Jie Hao[†,‖], Hanjie Jiang[†], Paul M. Zimmerman[†], Jinsang Kim*[,†,‡,§,○]

[†]*Department of Chemistry,* [‡]*Macromolecular Science and Engineering,* [§]*Department of Materials Science and Engineering, and* [○]*Department of Chemical Engineering, University of Michigan, Ann Arbor, Michigan, 48109, United States.*

[‖]*Center of Single-Molecule Sciences, Institute of Modern Optics, College of Electronic Information and Optical Engineering, Nankai University, China.*

**jinsang@umich.edu (J.K.)*

ABSTRACT

Metal-free organic triplet emitters are an emerging class of organic semiconducting material. Among them, molecules with tunable emission responsive to environmental stimuli have shown great potentials in solid state lighting, sensors, and anticounterfeiting systems. Here, a novel excited-state intramolecular proton transfer (ESIPT) system is proposed showing the activation of thermally activated delayed fluorescence (TADF) or room-temperature phosphorescence (RTP) simultaneously from both keto and enol tautomers. The prototype ESIPT triplet emitters exhibited up to 50% delayed emission quantum yield. Their enol-keto tautomerization can be switched by controlling the matrix acidity in doped polymer films. Taking advantage of these unique properties, we have devised "on-off" switchable triplet emission systems controlled by acid vapor annealing, as well as photopatterning systems capable of generating facile and high-contrast emissive patterns.

KEYWORDS

Metal-free organic triplet emitters, excited-state intramolecular proton transfer, thermally activated delayed fluorescence, room-temperature phosphorescence, switchable triplet emission systems

INTRODUCTION

Metal-free purely organic triplet emitters utilizing room-temperature phosphorescence (RTP)[1-3] or thermally activated delayed fluorescence (TADF)[4] are the functional components in modern technologies such as displays, solid-state lighting, and sensors. Over inorganic counterparts, these materials have many advantages such as a large design window, readily tunable properties, easy processability, and economic material cost.[5] Among them, emitters with tunable emission that can respond to environmental stimuli have attracted widespread attention.[6]

In conventional fluorescence emitters, one way to achieve tunable emission is through excited-state intramolecular proton transfer (ESIPT), which is a unique four-level photophysical process - while chromophores originally reside in their enol ground state (E), upon excitation to the excited enol form (E*), they undergo rapid tautomerization to an energetically lower excited keto configuration (K*), followed by emission to the keto ground state (K).[7] Importantly, the transient proton transfer process is highly sensitive to environmental stimuli, and frustrated proton transfer is widely observed in protic or polar environment.[8–10] With fine tuning of the structure and matrix, partially frustrated proton transfer has led to dual and triple ESIPT emitters[11] and even single molecule white emitters.[12–15]

This intriguing four-level photocycle and its unique sensitivity to environmental stimuli have inspired us to devise ESIPT-based triplet emitters and create stimuli-responsive systems with tunable triplet emission activated both in enol and keto forms. Harvesting triplet excitons from ESIPT chromophores is a generally overlooked field due to the insufficient molecular design blueprint. Table S1 listed out the reported ESIPT materials with room-temperature triplet emission. As TADF and RTP materials received wide attention in the past decade, recently, the intrinsic intramolecular charge transfer of ESIPT structures has been utilized to activate TADF in organic light-emitting devices,[16–18] followed by a few photophysical and computational study of their excited state dynamics.[19–21] On the other hand, however, activating RTP from ESIPT molecules is much less explored[22,23] while most photophysical studies focus on low-temperature phosphorescence properties.[24,25] Moreover, as these pioneering works explored the keto-form properties of ESIPT triplet emitters, molecular engineering pathways to harvest triplet energy from the enol tautomer is missing.

In this report, we created a series of organic triplet emitters having ESIPT properties in which efficient TADF or RTP with is activated both in enol and keto forms with a record-high delayed emission quantum yield up to 50%. Considering the complicated four-level

photocycle involved, the simplest (2′-hydroxyphenyl)benzimidazole (HBI, **1**) scaffold is chosen with subsequent attachment of Br to induce intramolecular heavy atom effect[26] and aromatic carbonyl as the El-Sayed-rule-satisfying unit[27] to create channels for orbital angular momentum migration.[28,29] This strategy is universally applicable to activating efficient triplet population from various ESIPT structures. A thorough photophysical study on the prototype molecules was conducted to elucidate the substitution effects of Br and carbonyl. We believe that future developments of triplet-activated ESIPT molecules would benefit from the outcome of this work.

Furthermore, the application merit of dual-form ESIPT triplet emitters was explored in the spirit of their sensitivity to acidity in the solid state matrices. These prototype materials exhibited "on-off" switchable enol-keto tautomerization in poly(4-vinylpyridine) (P4VP) with acid vapor annealing. Photo-reaction capabilities of the hydroxyl groups were also exploited to generate high-contrast emissive patterns utilizing the keto-enol photochromism.

RESULTS AND DISCUSSION

1. Molecular design and excited-state properties

In our design strategy, the key to triplet state activation of ESIPT molecules is creating transition channels between (π,π^*) and (n,π^*) states both in keto and enol forms, which potentially carry large spin-orbit coupling matrix elements (SOCMEs).[27] A computational study using the restricted active space - spin flip (RAS-SF) method[30–34] was performed to characterize the model compound HBI and determine the accessibility of these channels. RAS-SF is a wave function theory that is well-suited for treating electronically excited states.[35,36] Recent work has enabled RAS-SF to predict accurate SOC elements,[29] making it particularly useful to investigate the prototype ESIPT compounds.

Examination of the electronic transitions of HBI, as seen in the natural transition orbitals (NTO) (Figure S2), indicated that most low-energy excited states have primarily (π,π^*) character in both enol and keto forms. This is reflected in Figure 1a-b, where HBI molecules tend to show relatively low SOC constants, more specifically ~1.0 cm^{-1} for 1-enol and 1-keto, due to a lack of heavy atoms in singlet-triplet transitions. The T_2 state of 1-keto has significant (n,π^*) character and therefore moderate SOCME (~10 cm^{-1}) is expected in the S_1-T_2 transition, but the T_2 state is also significantly higher in energy than S_1 and therefore inaccessible.

To overcome the insufficient SOC in HBI, a carbonyl group was introduced to provide low energy (n,π^*) excited states and thus create accessible (π,π^*) - (n,π^*) transition channels exerting in-plane to out-of-plane orbital angular momentum rotation to facilitate SOC,[1,37] and Br was also introduced to elevate the overall SOCMEs. Specifically, Br is attached adjacent to carbonyl where its non-bonding electrons could participate in the carbonyl-centered n-π^* transition. This proximity results in much better utilization of the heavy atom effect compared to isolated Br and carbonyl,[38] in concordance with the heavy atom oriented orbital angular momentum manipulation effect (HAAM) we recently studied.[29]

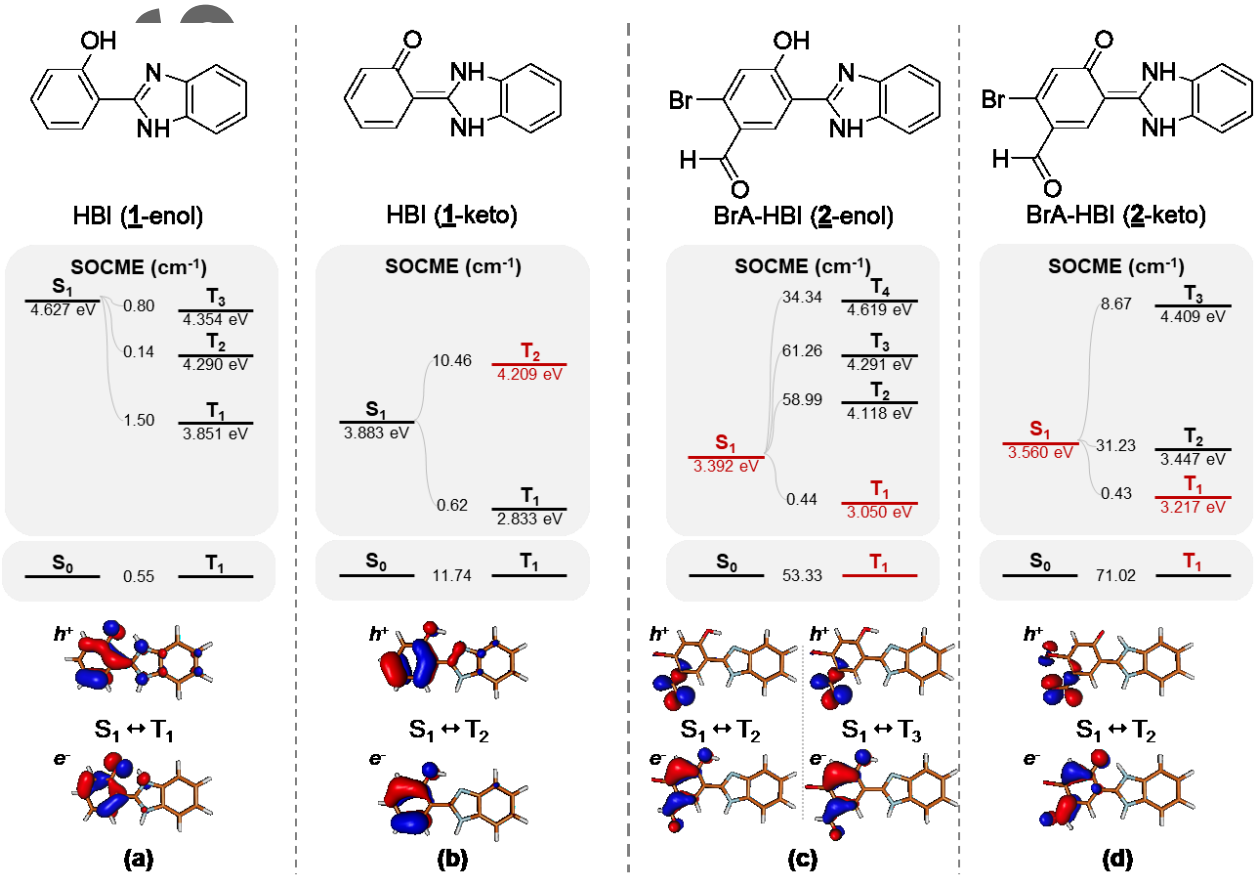

Figure 1. Chemical structures of HBI (**1**) and BrA-HBI (**2**) in their enol or keto forms; RAS-SF calculation results for the selected excited states (black denotes π,π^* while red denotes n,π^* states), their energies, and SOCMEs between S_1 and triplet states as well as that between S_0 and T_1. RAS-SF NTOs of selected S-T transitions are displayed. An expanded NTO table is shown in Figure S1. The orbital configuration of each state is shown in Figure S2.

The strategically created BrA-HBI (Figure 1c-d) with qualitatively distinct low-lying states compared to HBI, where the former's S_1 and T_1 states show considerable (n,π^*) character. In addition, the S_1 states of BrA-HBI have much lower excitation energy compared to that of HBI, corresponding to transitions between the non-bonding (n) and π^* orbitals (see

NTOs in Figure S1), given that lone-pair electron orbitals of aldehyde are higher in energy than electrons in the bonding π orbitals. Due to the low orbital overlap between the non-bonding and anti-bonding π^* orbitals, BrA-HBI have relatively small S_1-T_1 energy gaps, where $\Delta E_{S_1-T_1} \cong 0.34$ eV in both 2-enol and 2-keto, according to the energy diagram shown in Figure 1c-d.

While potential triplet emission channels are created by the aldehyde group, the plausibility of populating the T_n states still depends on additional factors. In 2-enol, the S_1-T_1 SOCME is low (Figure 1c) since S_1 and T_1 each has (n,π^*) character, and the T_2 state of 2-enol has a high excitation energy that makes it inaccessible. The keto tautomer, 2-keto, exhibits a lower-energy T_2 state than the enol tautomer, mainly due to the intrinsic C=O double bond that stabilizes the π^* orbital, which further lowers the transition energies between S_1 and T_2 states. This intrinsic carbonyl of the keto form helps create the efficient S_1-T_2 ISC channel with a high SOCME of 31.2 cm^{-1} that bears n to π orbital angular momentum variation (see the NTOs of BrA-HBI in Figure S1), which helps promote triplet population, and similarly significant T_1-S_0 SOC, stimulating triplet emission.

With these computational prediction and insights in hand, we conducted a series of photophysical studies to further validate the capabilities of the BrA-HBI.

2. Photophysical properties of BrA-HBI

In a diluted solution, BrA-HBI displayed characteristic keto emission with large Stokes shift (>60 nm from the onsets, Figure 2b). The emission peak was hypsochromically shifted upon increasing the solvent polarity. However, the ESIPT processes were efficient enough to prevent enol emission even in protic ethanol.

Triplet state properties of BrA-HBI in solid state were studied by doping it in poly(methyl methacrylate) (PMMA) and poly(acrylic acid) (PAA) separately. PMMA was chosen as a neutral host for the keto tautomer and PAA as an acidic host with the potential to hinder proton transfer process and unveil enol emission. As shown in Figure 2d, BrA-HBI in PMMA exhibited characteristic steady state emission in its keto form with a large Stokes shift. The total quantum yield (Φ_{tot}) rose from 9.8 % to 31 % from air to anoxic condition, which was accompanied by an increased delayed emission lifetime (τ_d) to 1.90 ms (Figure 2c), indicating considerable contribution from triplet excitons. Unexpectedly, the delayed and stead-state emission profile almost coincide with each other, suggesting potential TADF emission character but with a rather slow room-temperature lifetime in the ms regime.

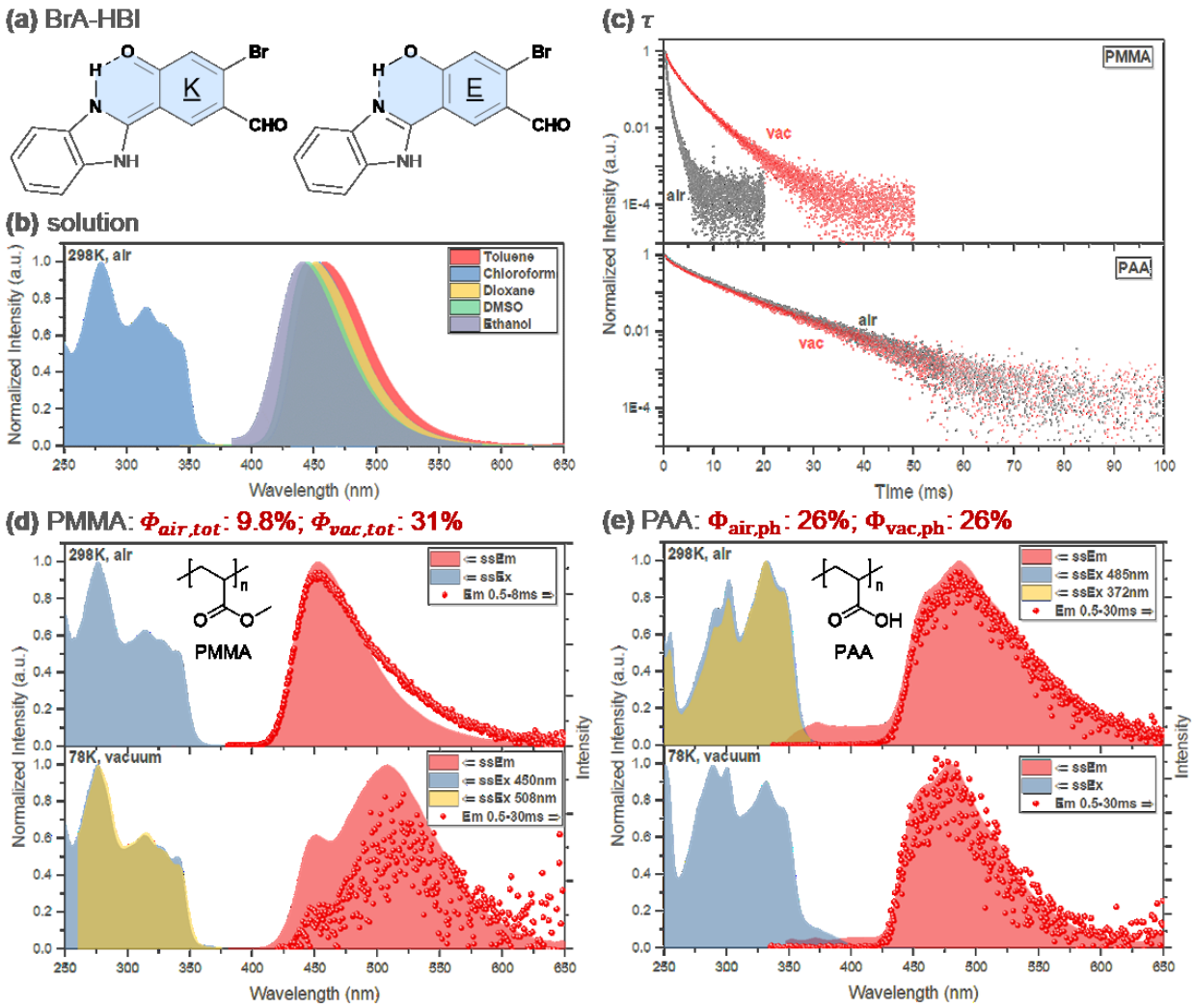

Figure 2. (a) Chemical structure of BrA-HBI in its enol (E) and keto (K) form; steady state excitation (filled), emission spectra (filled), and delayed emission spectra (dots) of BrA-HBI in (b) various solvents (OD~0.1) at 298 K, spin-coated (d) PMMA or (e) PAA films with 1 wt% doping concentration measured at 298 K (top) and 78 K (bottom); (c) emission decay curves of BrA-HBI in PMMA (top) or PAA (bottom) measured at 298 K in air or in vacuum, which were measured from 200 μs.

Temperature-variant experiments were then performed to study the origin of the emission. As the temperature dropped to 78 K, a new lower-energy peak emerged near 508 nm while the emission band at ca. 450 nm gradually faded (Figure 2d, S5). The new emission peak near 508 nm could be characterized as phosphorescence emission while the original emission band at higher temperature could be assigned to a mixture of prompt fluorescence and TADF emission. Besides, the τ_d v.s. T curve were also recorded in Figure S5 which suggested the migration between two lifetime species (i.e. TADF and phosphorescence). These verifications strongly supported the TADF nature of the emission at room temperature with a ΔE_{ST} of 0.31 eV (from the emission peak, or λ_{max} at 78 K).

Computational results (Figure 1) provide a plausible explanation for the emission mechanism. Although carbonyl attachment has created a new S_1/T_1 pair with (n,π^*) and thus mild charge transfer (CT) character, the gap (0.34 eV) is large, not to mention the low S_1-T_1 SOCME of ca. 0.2 cm^{-1}. However, we suspect that the up-conversion of triplet excitons may be assisted by the T_2 state and the S_1-T_2 ISC channel with considerable SOCME, possibly through the spin-vibronic coupling pathway[39–43] as demonstrated in some blue TADF emitters.[44]

Interestingly in the doped PAA system (Figure 2e), we observed a completely different emission profile with a new higher-energy fluorescence band below 400 nm, which overlaps with the excitation spectrum, indicating a small Stokes shift typically seen in the enol tautomer. The room temperature delayed emission spectrum displayed a structured profile and maintained its shape at 78 K with only a small hypsochromic shift. Together with the single-component decay profile of τ_d v.s. T curve (Figure S6), this indicates that BrA-HBI in PAA exhibited phosphorescence emission character instead, in sharp contrast to its TADF character in PMMA matrix.

To confirm the enol emission in PAA, we permanently blocked ESIPT through methylation on the hydroxyl group of BrA-HBI. When the resulting molecule was doped into PMMA and PAA, both systems displayed a similar emission profile to that of BrA-HBI@PAA system with a fluorescence band below 400 nm and a phosphorescence band at ca. 520 nm (Figure S7). Thus, we confirmed the blocked ESIPT of BrA-HBI in PAA matrix, most likely due to the strong solid-state intermolecular H-bond interaction between PAA and the phenolic ESIPT donor on BrA-HBI.

3. Dissecting the substitution effects of Br and carbonyl

In general, carbonyl substitution is considered essential to generate low-energy non-bonding electrons that assist in the orbital angular momentum shift,[28] in line with the El-Sayed rule;[27] meanwhile, Br is used to boost the overall SOC efficiencies. Further verification of their effects under our molecular scaffold was conducted by comparing the photophysical properties of BrA-HBI to those of mono-functionalized Br-HBI (with Br only) and A-HBI (with aldehyde only), as well as the non-functionalized HBI. Their properties in PMMA or PAA matrices are separately discussed as follows.

In PMMA (Figure 3a-c), non-functionalized HBI itself displayed classical keto emission without any delayed contents. Triplet emission was spotted in the form of TADF with aldehyde attachment. On the other hand, Br mono-substituted Br-HBI displayed three peaks

in its delayed emission profile. While the other two (486 and 530 nm) could be assigned to phosphorescence emission from T_1 state, the one at the higher energy (460 nm) likely originated from T_2 phosphorescence and contained minimal TADF character since its intensity relative to T_1 phosphorescence does not decrease even at 78 K.

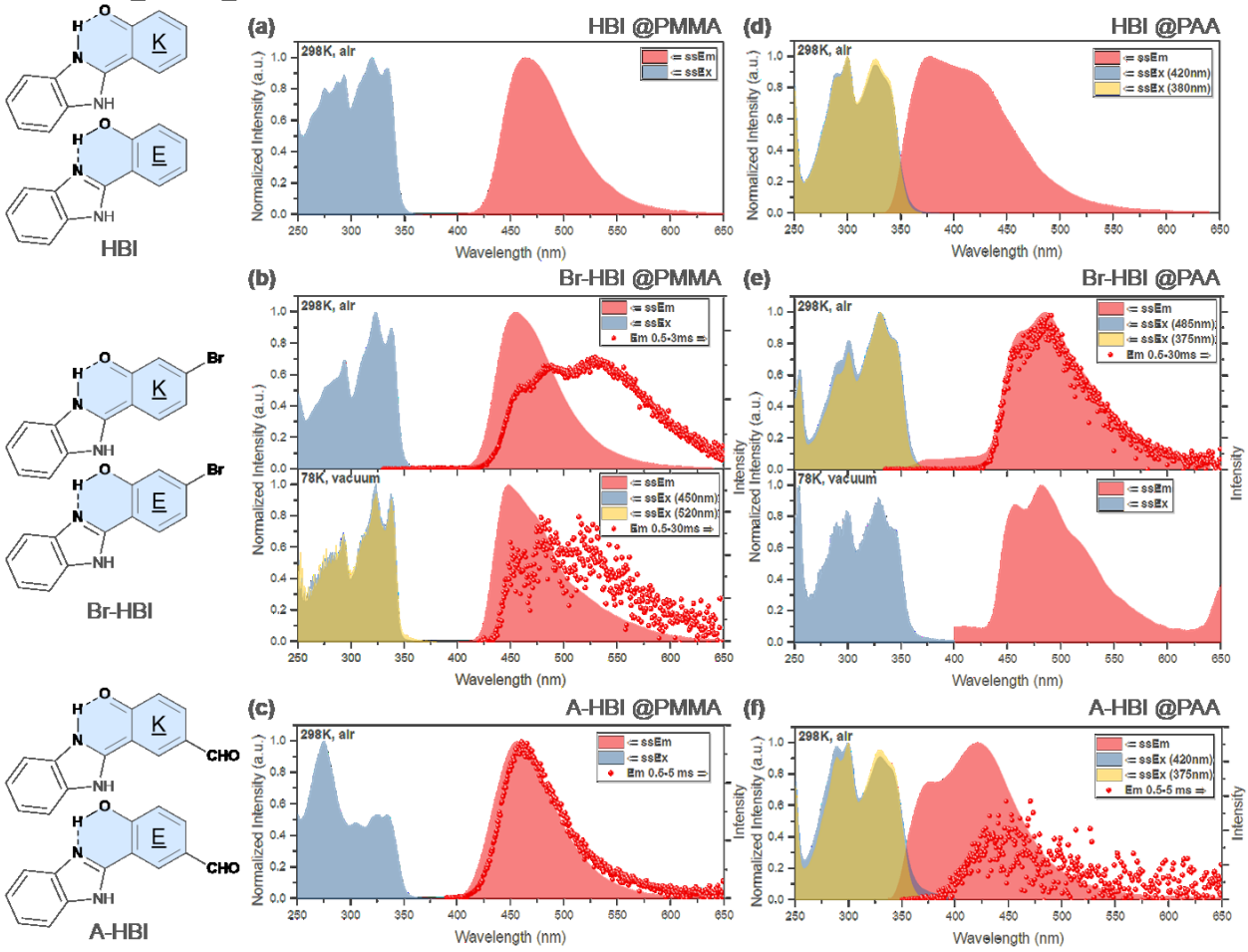

Figure 3. Steady state excitation (filled), emission spectra (filled), and delayed emission spectra (dots) of HBI, Br-HBI, and A-HBI in spin-coated (a-c) PMMA or (d-f) PAA films with 1 wt% doping concentration measured at 298 K or 78 K (indicated in each figure).

However, Br attachment alone in the absence of aldehyde is not sufficient to upconvert triplet excitons to singlet domains; thus, its delayed spectrum mostly consists of phosphorescence emission as the emission λ_{max} is independent of temperature change. To achieve quantitative comparison, we then deconvoluted the total quantum yield of each emitter into prompt and delayed portions. While the delayed and steady-state profile couldn't be spectrally separated, we managed to extract the delayed contents by analyzing the lifetime and steady state emission profiles in air vs. anoxic conditions (see section V in SI for details).

As shown in Figure 4a, aldehyde substituted A-HBI dramatically enhanced the delayed QY to 14%, while Br substituted Br-HBI only displayed 6% Φ_{delay}. These results are

expected from the calculated keto-form energy state and SOCME profile (Figure S3): aldehyde substitution alone could create new S_1 and T_1 states with (n,π^*) character and thus efficient $(n,\pi^*) \rightarrow (\pi,\pi^*)$ ISC channels for triplet population, while Br-HBI, despite its globally enhanced SOC, lacks efficient down-converting ISC channels due to its significantly large S_1-T_1 energy gap and inefficient SOCMEs. However, additional Br attachment on top of aldehyde substitution enhanced further the overall SOC efficiency (as calculated) as well as Φ_{delay} (14 to 26%).

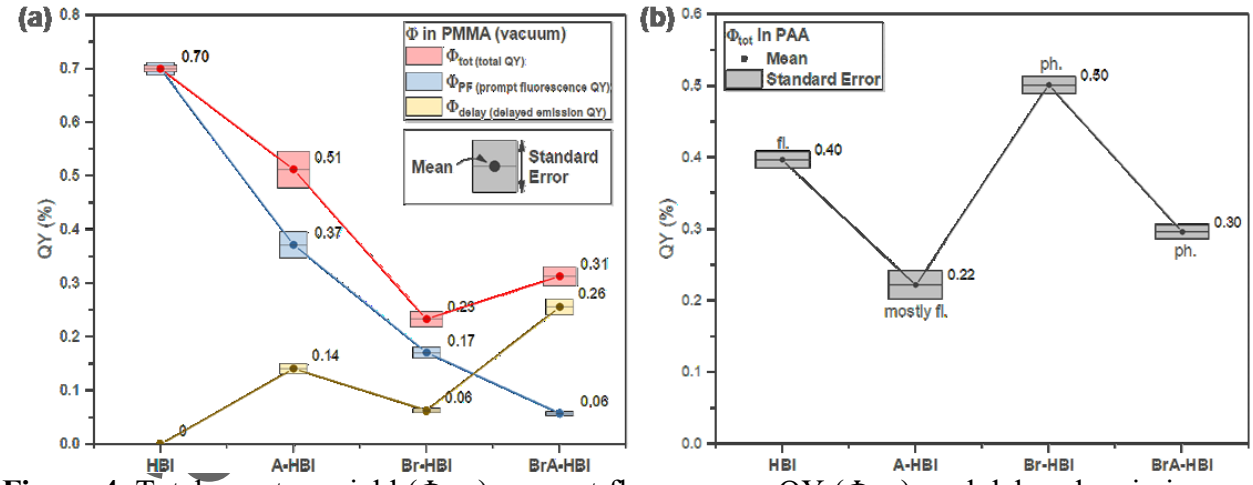

Figure 4. Total quantum yield (Φ_{tot}), prompt fluorescence QY (Φ_{PF}), and delayed emission QY (Φ_{delay}) of HBI, A-HBI, Br-HBI, and BrA-HBI measured in (a) PMMA and (b) PAA.

On the other hand, prompt fluorescence QY (Φ_{PF}) dropped dramatically from HBI (as high as 70%) through A/Br-HBI to BrA-HBI (6%). Although aldehyde attachment in A-HBI incited large Φ_{delay}, the total QY (Φ_{tot}), compared to unsubstituted HBI, still dropped to 53% likely due to increased non-radiative decay from long-lived triplet excitons. It is surprising that, potentially due to efficient triplet population, Br attachment alone would lead to large drop in Φ_{tot} to 23%, which was eventually recovered to 31% in fully-armed BrA-HBI. Interpreted from the computational results (Figure S3), adequate S_1-T_2 exciton up-conversion may be activated in Br-HBI, but the large $\Delta E_{T_2-T_1}$ may not be favorable for the relaxation of high-energy triplet excitons. As a result, some T_2 excitons could directly relax to ground state as the spectrum indicated (Figure 3b), and a few percent of T_2 electrons survived to T_1 state and emitted regular phosphorescence according to Kasha's rule.[45]

In PAA, while all four emitters displayed characteristic enol emission (Figure 3d-f), Br substitution played critical role to induce large phosphorescence yield (Φ_{ph}, Figure 4b). Predicted from the calculation results for the enol-form (Figure S4), all four emitters were not expected to exhibit large triplet population: efficient SOC channel is missing in HBI and

Br-HBI since the lowest energy states have pure (π,π^*) character; despite having new (n,π^*) S_1 and T_1 states, the aldehyde-equipped A-HBI and BrA-HBI still lack an efficient SOC channel due to the higher lying $^3(\pi,\pi^*)$ T_2 states (ca. 4.1 eV) v.s. S_1 states (ca. 3.4 eV). This is reflected in the emission profile of HBI and A-HBI where except for the weak delayed emission in A-HBI, both emitters displayed mostly prompt fluorescence in PAA. However, Br attachment brought up major discrepancy: while almost pure phosphorescence was achieved in the BrA-HBI@PAA system with a high Φ_{ph} of 30%, Br attachment alone reached an even higher Φ_{ph} of 50% in PAA (Figure 4b).

The exact origin of this unexpectedly high Φ_{ph} is unknown but may shine light on the benefit of PAA as a great yet overlooked matrix for triplet emitters: 1) due to the large density of H-bonds in PAA, it serves as a good oxygen barrier. In PAA, τ_{ph} in air is almost the same as that in anoxic conditions, which is quite the opposite in PMMA (Figure 2c); 2) PAA could establish multiple H-bonds with our ESIPT molecules, which helps prevent triplet excitons from decaying non-radiatively – a strategy widely used in organic RTP emitters;[46–48] 3) The presented results suggest a potential synergic effect between Br and PAA with the enol form only. We are currently reviewing the origin of this effect.

In short, we systematically analyzed the substituent effects of Br and aldehyde in promoting triplet population and delayed emission in this section through discussing the photophysical properties of HBI, Br-HBI, and A-HBI in PMMA and PAA. The results in PMMA are in good agreement with prediction: carbonyl is used to create channels for orbital angular momentum change during SOC, while Br is used to boost the overall SOC efficiencies. In PAA, however, Br is critically important to induce efficient triplet emission due to promising external effects from the PAA matrix.

4. On-off switchable ESIPT systems in response to acid vapor

The switchable ESIPT process in PMMA vs. PAA instigated us to develop smart responsive systems. Poly(4-vinylpyridine) (P4VP) was selected since, despite being neutral, it is readily pronated upon acid doping[49] and serves as an acidic matrix. As for the ESIPT chromophore, we selected Br-HBI instead of BrA-HBI since its emissive species is easily distinguishable due to very high Φ_{ph} in its enol form but very low triplet yield in its keto form.

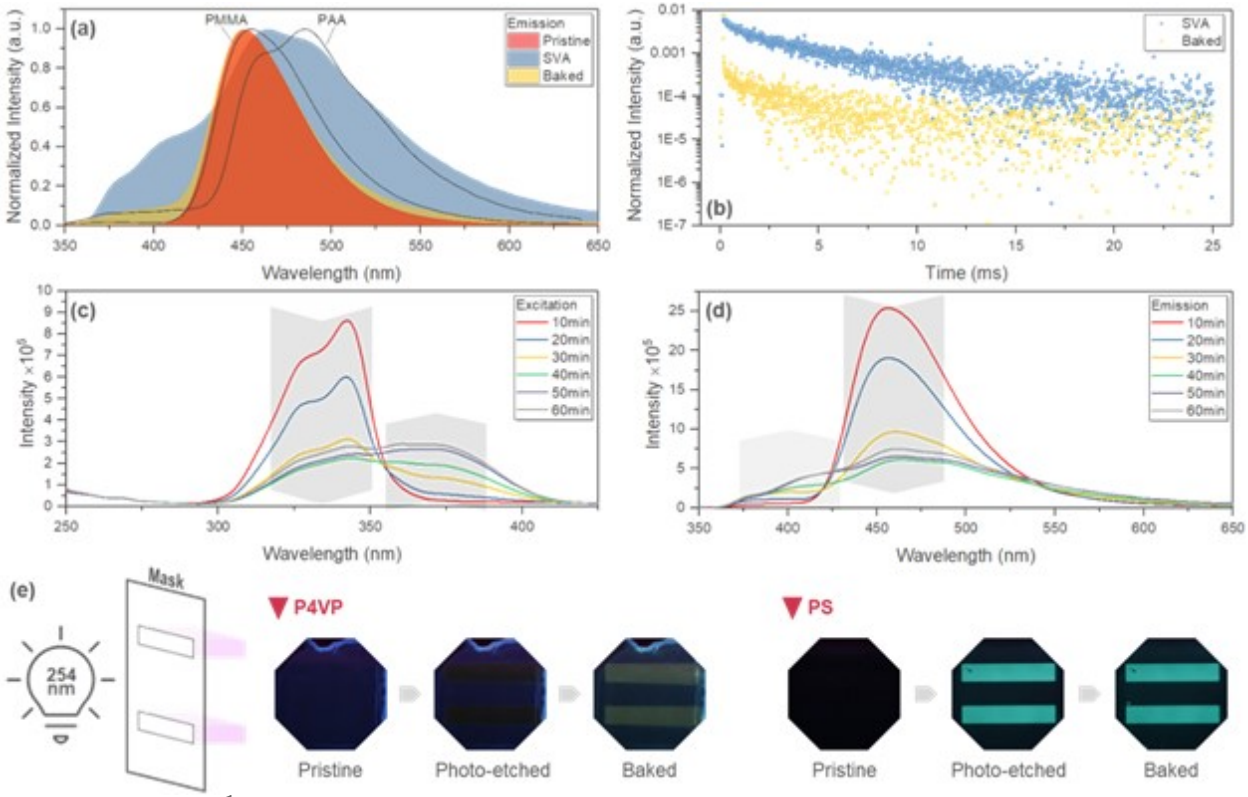

Figure 5. (a) Normalized steady state emission spectra (filled) and (b) emission decay curves (dots) of Br-HBI in P4VP (spin-coated, 1 wt% doping) upon solvent vapor annealing (SVA) with concentrated HCl and subsequent baking. Emission spectra in PMMA and in PAA (line) are included in for reference. The decay curves were measured from 0 ms. (c) excitation spectra and (d) steady state emission as SVA progressed. (e) Emissive patterns of Br-HBI in P4VP or PS under 365 nm illumination created by photo-etching with 254 nm UV lamp and a mask, followed by baking at 150°C (P4VP) or 60°C (PS).

The Br-HBI@P4VP film was subjected to solvent vapor annealing (SVA) with concentrated HCl. As shown in Figure 5a, keto emission was detected from the pristine film which well resembled that from PMMA. Upon acid treatment, P4VP was protonated, and the emission profile shifted to the enol species with a rising high energy (<400 nm) fluorescence band, similar to that in PAA. Furthermore, original keto emission was recovered when the films were baked, possibly due to the evaporation of HCl[49] and consequent deprotonation of P4VP. These results indicate certain reversibility in our system.

As expected, in the protonated P4VP, Br-HBI exhibited much longer-lived phosphorescence (Figure 5b), indicating strong host-guest interactions in the protonated film, which can effectively suppress the non-radiative decay. Additionally, Figure 5c-d show the gradual keto-enol migration of the active emissive species upon the acid vapor treatment, during which an unexpected new excitation band emerged at a lower energy (ca. 370 nm). Although we cannot clearly identify the new excitation species, it could originate from the strong host-guest interaction.

Furthermore, the keto-enol switching in P4VP indeed originated from matrix acidity variation instead of direct protonation of the ESIPT molecule, which is supported by the SVA performance in the inert polystyrene (PS) matrix (Figure S8). Only mild intensity drop was observed in the emission profile of PS film upon acid vapor annealing, and the emission stays in the keto form.

5. Photopatterning and photochromism

Triplet emission chromism during enol-keto exchange has inspired us to explore their photopatterning applications. It turns out that keto-to-enol tautomerization is directly achievable upon photochemical etching with 254 nm UV, which is capable of generating phenoxy radicals from the hydroxyl moieties in the ESIPT molecules,[50] which then react with the polymer backbone and block the proton transfer processes. This is accompanied by a distinct emission color change from blue to yellowish-green under 365 nm UV excitation.

As shown in Figure 5e and S9-10, Br-HBI was doped in P4VP or PS and the resulting thin films were subjected to 254 nm photochemical etching under a mask. In P4VP, the irradiated area displayed faint yellow-green color which became much brighter after subsequent baking. The pattern was stable after long-term storage. In PS, under the same fabrication conditions, much brighter green emission pattern was revealed after UV irradiation but additional thermal annealing had minimal effect. Photophysical analysis exhibited considerable triplet emission character from the treated areas (Figure S11), indicating enol emission since keto-form Br-HBI could not emit long-lived photons in the yellowish-green regime. Under 365 nm excitation, the generated photopatterns displayed high contrast to non-treated areas, which benefited from the fact that a new excitation band emerged past 365 nm in the treated sample while the pristine film has minimum absorption at 365 nm (Figure S11).

CONCLUSIONS

ESIPT molecules have intriguing four-level photophysical states, but they have been rarely used as triplet emitters. The acid sensitivity of proton transfer process has inspired us to develop ESIPT based metal-free organic triplet emitters exhibiting switchable dual-form emission. We started from the simplest HBI structure and successfully activated bright room-temperature triplet emission both in the keto and enol tautomers by incorporating aldehyde to generate efficient $(n,\pi^*)-(\pi,\pi^*)$ SOC channels and Br to elevate the overall SOC efficiencies. Interestingly, the developed BrA-HBI is capable of emitting blue delayed fluorescence in its keto form with a high Φ_d of 31% in PMMA, while enol-related green

phosphorescence is detected in PAA with 26% Φ_{ph}. We further investigated the effect of Br and aldehyde, separately, on triplet population and triplet emission. Results highlighted unexpected external boosting effects of PAA host on the phosphorescence efficiency of brominated ESIPT chromophores. Surprisingly, enol-form Br-HBI exhibited 50% Φ_{ph} in PAA matrix. To our best knowledge, BrA-HBI and Br-HBI were among the brightest ESIPT triplet emitters designed so far (SI).

Application merits of the prototype ESIPT triplet emitters were explored in the spirit of the keto-enol tautomerization. We have developed on-off switchable system that is responsive to acid vapor by utilizing reversibly protonation of P4VP matrix. Upon switching the matrix acidity, ESIPT triplet emitters could undergo switching between their enol and keto forms. Secondly, photo-patterning systems were developed by taking advantage of the triplet emission chromism of ESIPT chromophores. Bright yellowish-green emissive patterns were generated with high contrast.

In summary, we activated bright triplet emission from conventional ESIPT chromophores and exploited the enol-keto "on-off" switchability in various materials systems. The simplicity of our material design and the comprehensive photophysical investigation may allow for the future developments of ESIPT triplet emitters and their advances in solid-state lighting, information encryption, and solid-state sensors.

SUPPLEMENTAL INFORMATION

The Supporting Information includes the following: additional experimental details, computational details, additional photophysical analyses, protocol for extracting delayed emission quantum yield from total quantum yield, RAS-SF frontier molecular orbitals of the prototype molecules, and NMR spectra.

AUTHOR CONTRIBUTIONS

W.S. designed this manuscript. Preliminary calculation was conducted by W.S.. RAS-SF calculation was conducted by H.J.. Computational results were analyzed by W.S. and H.J.. Synthetic route of the molecules studied was desined by W.S. and J.H.; J.H. synthesized Br-HBI, BrA-HBI, A-HBI, while W.S. conducted the methylation of BrA-HBI. The rest of the experiments, including photophysical analyses, SVA, and photopatterning, was conducted by W.S.. P.M.Z. supervised the computational investigation. J.K. supervised the the overall manuscript.

ACKNOWLEDGMENTS

We acknowledged the financial support from National Science Foundation (DMREF DMR 1435965) and Samsung Global Research Outreach.

ADDITIONAL INFORMATION

The authors declare no competing financial interests. Further information and requests for the data that support the findings of this study should be directed to and will be fulfilled by the corresponding author, Jinsang Kim (jinsang@umich.edu).

REFERENCES

[1] O. Bolton, K. Lee, H. J. Kim, K. Y. Lin, J. Kim, *Nature Chemistry* **2011**, *3*, 205.

[2] Z. An, C. Zheng, Y. Tao, R. Chen, H. Shi, T. Chen, Z. Wang, H. Li, R. Deng, X. Liu, W. Huang, *Nature Materials* **2015**, *14*, 685.

[3] D. Lee, O. Bolton, B. C. Kim, J. H. Youk, S. Takayama, J. Kim, *Journal of the American Chemical Society* **2013**, *135*, 6325.

[4] H. Uoyama, K. Goushi, K. Shizu, H. Nomura, C. Adachi, *Nature* **2012**, *492*, 234.

[5] S. Mukherjee, P. Thilagar, *Chemical Communications* **2015**, *51*, 10988.

[6] N. A. Kukhta, M. R. Bryce, *Materials Horizons* **2021**, *8*, 33.

[7] V. S. Padalkar, S. Seki, *Chemical Society Reviews* **2016**, *45*, 169.

[8] D. McMorrow, M. Kasha, *Journal of the American Chemical Society* **1983**, *105*, 5133.

[9] Michael Kasha, *Journal of the Chemical Society, Faraday Transactions 2: Molecular and Chemical Physics* **1986**, *82*, 2379.

[10] M. H. van Benthem, G. D. Gillispie, *Journal of Physical Chemistry* **1984**, *88*, 2954.

[11] J. Massue, D. Jacquemin, G. Ulrich, *Chemistry Letters* **2018**, *47*, 1083.

[12] E. Heyer, K. Benelhadj, S. Budzák, D. Jacquemin, J. Massue, G. Ulrich, *Chemistry - A European Journal* **2017**, *23*, 7324.

[13] K. Benelhadj, W. Muzuzu, J. Massue, P. Retailleau, A. Charaf-Eddin, A. D. Laurent, D. Jacquemin, G. Ulrich, R. Ziessel, *Chemistry - A European Journal* **2014**, *20*, 12843.

[14] K. Tang, M. Chang, T. Lin, … H. P.-J. of the, undefined 2011, *ACS Publications* **2011**, *133*, 17738.

[15] S. Haldar, D. Chakraborty, B. Roy, G. Banappanavar, K. Rinku, D. Mullangi, P. Hazra, D. Kabra, R. Vaidhyanathan, *Journal of the American Chemical Society* **2018**, *140*, 13367.

[16] K. Wu, T. Zhang, Z. Wang, L. Wang, L. Zhan, S. Gong, C. Zhong, Z. H. Lu, S. Zhang, C. Yang, *Journal of the American Chemical Society* **2018**, *140*, 8877.

[17] M. Mamada, K. Inada, T. Komino, W. J. Potscavage, H. Nakanotani, C. Adachi, *ACS Central Science* **2017**, *3*, 769.

[18] A. K. Gupta, W. Li, A. Ruseckas, C. Lian, C. L. Carpenter-Warren, D. B. Cordes, A. M. Z. Slawin, D. Jacquemin, I. D. W. Samuel, E. Zysman-Colman, *ACS Applied Materials and Interfaces* **2021**, *13*, 15459.

[19] Y. Long, M. Mamada, C. Li, P. L. dos Santos, M. Colella, A. Danos, C. Adachi, A. Monkman, *Journal of Physical Chemistry Letters* **2020**, *11*, 3305.

[20] A. S. Berezin, K. A. Vinogradova, V. P. Krivopalov, E. B. Nikolaenkova, V. F. Plyusnin, A. S. Kupryakov, N. v. Pervukhina, D. Y. Naumov, M. B. Bushuev, *Chemistry - A European Journal* **2018**, *24*, 12790.

[21] Y. Cao, J. Eng, T. J. Penfold, *Journal of Physical Chemistry A* **2019**, *123*, 2640.

[22] R. M. Khisamov, A. A. Ryadun, T. S. Sukhikh, S. N. Konchenko, *Molecular Systems Design & Engineering* **2021**.

[23] F. Liang, L. Wang, D. Ma, X. Jing, F. Wang, *Applied Physics Letters* **2002**, *81*, 4.

[24] D. Sahoo, T. Adhikary, P. Chowdhury, S. C. Roy, S. Chakravorti, *Chemical Physics* **2008**, *352*, 175.

[25] M. Hagiri, N. Ichinose, J. I. Kinugasa, T. Iwasa, T. Nakayama, *Chemistry Letters* **2004**, *33*, 326.

[26] H. Saigusa, T. Azumi, *The Journal of Chemical Physics* **2008**, *71*, 1408.

[27] M. A. El-Sayed, *The Journal of Chemical Physics* **1963**, *38*, 2834.

[28] N. J. Turro, V. Ramamurthy, J. C. Scaiano, *Modern Molecular Photochemistry of Organic Molecules*, First Indi., Vol. 88, University Science Books, Sausalito, CA, **2012**.

[29] W. Shao, H. Jiang, R. Ansari, P. Zimmerman, J. Kim, *Chemical Science* **2022**, *13*, 789.

[30] A. D. Chien, P. M. Zimmerman, *Journal of Chemical Physics* **2017**, *146*, 014103.

[31] F. Bell, P. M. Zimmerman, D. Casanova, M. Goldey, M. Head-Gordon, *Physical Chemistry Chemical Physics* **2013**, *15*, 358.

[32] P. M. Zimmerman, F. Bell, M. Goldey, A. T. Bell, M. Head-Gordon, *Journal of Chemical Physics* **2012**, *137*, 164110.

[33] H. Jiang, P. M. Zimmerman, *Journal of Chemical Physics* **2020**, *153*, 064109.

[34] D. Casanova, M. Head-Gordon, *Physical Chemistry Chemical Physics* **2009**, *11*, 9779.

[35] A. I. Krylov, *Chemical Physics Letters* **2001**, *338*, 375.

[36] A. I. Krylov, *Chemical Physics Letters* **2001**, *350*, 522.

[37] H. Ma, Q. Peng, Z. An, W. Huang, Z. Shuai, *Journal of the American Chemical Society* **2019**, *141*, 1010.

[38] S. Sarkar, H. P. Hendrickson, D. Lee, F. Devine, J. Jung, E. Geva, J. Kim, B. D. Dunietz, *Journal of Physical Chemistry C* **2017**, *121*, 3771.

[39] J. Gibson, A. P. Monkman, T. J. Penfold, *ChemPhysChem* **2016**, 2956.

[40] E. W. Evans, Y. Olivier, Y. Puttisong, W. K. Myers, T. J. H. Hele, S. M. Menke, T. H. Thomas, D. Credgington, D. Beljonne, R. H. Friend, N. C. Greenham, *Journal of Physical Chemistry Letters* **2018**, *9*, 4053.

[41] J. Gibson, T. J. Penfold, *Physical Chemistry Chemical Physics* **2017**, *19*, 8428.

[42] I. Kim, S. O. Jeon, D. Jeong, H. Choi, W. J. Son, D. Kim, Y. M. Rhee, H. S. Lee, *Spin-Vibronic Model for Quantitative Prediction of Reverse Intersystem Crossing Rate in Thermally Activated Delayed Fluorescence Systems*, Vol. 16, **2020**, pp. 621–632.

[43] M. K. Etherington, J. Gibson, H. F. Higginbotham, T. J. Penfold, A. P. Monkman, *Nature Communications* **2016**, *7*, 1.

[44] T. Hosokai, H. Noda, H. Nakanotani, T. Nawata, Y. Nakayama, H. Matsuzaki, C. Adachi, *Journal of Photonics for Energy* **2018**, *8*, 1.

[45] M. Kasha, *Discussions of the Faraday Society* **1950**, *9*, 14.

[46] Y. Zhu, Y. Guan, Y. Niu, P. P. P. Wang, R. Chen, Y. Wang, P. P. P. Wang, H. lou Xie, *Advanced Optical Materials* **2021**, *2100782*, 1.

[47] M. S. Kwon, Y. Yu, C. Coburn, A. W. Phillips, K. Chung, A. Shanker, J. Jung, G. Kim, K. Pipe, S. R. Forrest, J. H. Youk, J. Gierschner, J. Kim, *Nature Communications* **2015**, *6*.

[48] M. S. Kwon, D. Lee, S. Seo, J. Jung, J. Kim, *Angewandte Chemie* **2014**, *126*, 11359.

[49] T. Ma, T. Li, L. Zhou, X. Ma, J. Yin, X. Jiang, *Nature Communications* **2020**, *11*, 1.

[50] S. Zhao, H. Ma, M. Wang, C. Cao, J. Xiong, Y. Xu, S. Yao, *Photochemical and Photobiological Sciences* **2010**, *9*, 710.

A novel excited-state intramolecular proton transfer (ESIPT) system is presented exhibiting thermally activated delayed fluorescence or room-temperature phosphorescence simultaneously from keto or enol tautomers, respectively. These ESIPT triplet emitters show up to 50% delayed emission quantum yield and acidity-responsive switchable tautomerization. Unique “on-off” switchable triplet emission controlled by acid vapor annealing as well as high-contrast photopatterning systems are demonstrated.